Smart Weed-Crop Classification in Winter Wheat Fields: A Deep Learning Approach for Sustainable Agriculture

S. I. Saedi[1*], H. Makarian[2]

1- Department of Water and Soil, Faculty of Agriculture, Shahrood University of Technology, Shahrood, Iran
2- Department of Agronomy and Plant Breeding, Faculty of Agriculture, Shahrood University of Technology, Shahrood, Iran
(*- Corresponding Author Email: isaedi@shahroodut.ac.ir)
https://doi.org/10.22067/jam.2026.97533.1467

Abstract

Improving wheat productivity is essential for maintaining food security in the coming years. A major challenge to wheat production is the presence of weeds, which can greatly reduce its yield. In this context, precision weed management based on weed-crop classification can be a key factor for achieving sustainable wheat production. To accomplish this goal, in the present study, we utilised colour images and deep learning techniques to distinguish winter wheat from four prevalent weeds, creating five distinct classes. Four deep learning networks–Xception, EfficientNetB0, VGG19, and InceptionResNetV2–were evaluated to serve as backbone networks to fulfil the classification requirements. These networks were pre-trained on ImageNet using transfer learning, then enhanced with additional layers to improve performance on our dataset. The improved InceptionResNetV2 model demonstrated the highest performance among the four models, achieving an accuracy of 98.17% and a loss of 3.19% on the test data. Nevertheless, all models demonstrated excellent performance in distinguishing plant classes, achieving weighted average F1-scores of 97%, 86%, 94%, and 98% for the improved models based on Xception, EfficientNetB0, VGG19, and InceptionResNetV2, respectively. Additionally, we analysed fifteen scenarios of weed presence in winter wheat fields, focusing on various weed types studied, to propose effective weed management strategies utilising the four models. The research findings provide a foundation for developing mobile apps or robotic weeders that facilitate site-specific weed management. This approach aims to reduce herbicide use and environmental impact while also improving wheat yield and quality.

Keywords: Deep learning, RGB image, Weed recognition, Winter wheat

Introduction

As the global population continues to grow, wheat emerges as a vital crop in addressing the world's increasing nutritional demands (Sadeghi, Saedi, Peters, & Stöckle, 2022; Saedi, Alimardani, Mousazadeh, & Salehi, 2019; Shewry & Hey, 2015). Wheat plays a key role in global food security, supplying roughly 20% of the essential carbohydrates and proteins needed for human consumption (Langridge *et al.*, 2022). It occupies about 30% of the world's cereal cropland, underscoring its critical importance in agricultural systems (FAO, 2021). In light of the increasing challenges posed by climate change and a rapidly growing global population, enhancing wheat productivity has emerged as a crucial strategy to uphold food security in the years ahead. One significant obstacle to wheat production is weeds, which reduce the growth and yield of wheat by competing for water, nutrients, and light (Singh, Kukal, Irmak, & Jhala, 2021). Weeds can significantly affect wheat productivity, with estimated yield losses of up to 30%, largely influenced by varying climatic conditions and differences in agricultural management practices (Gyawali, Bhandari, Budhathoki, & Bhattarai 2022). In many of Iran's key wheat-producing areas, broadleaved weeds have emerged as a prominent concern, accounting for a staggering 84% of the weed species infesting wheat fields and posing a significant threat to crop yields (Montazeri, Zand, & Baghestani, 2005). Manual removal of weeds in wheat fields is not a viable option due to the risk of crop damage and the high labour costs involved. Precise identification and differentiation of weeds from crop plants is a crucial component of effective site-specific weed management. By accurately distinguishing weeds from wheat, farmers can target herbicide applications to specific areas where weeds are present, thereby optimising weed control.

By harnessing the power of advanced technologies such as computer vision and image processing, researchers can achieve high precision in weed detection, enabling the development of targeted management strategies that accurately distinguish between crops and weeds, ultimately optimising the effectiveness of site-specific weed control techniques (Juwono *et al.*, 2023). Through providing two-dimensional information, colour images have been widely utilised in this domain, laying the groundwork for further advancements. Studies have shown that unique morphological characteristics, including leaf form, colour, and dimension, can serve as valuable features for object recognition and classification tasks (Susetyarini, Wahyono, Latifa, & Nurrohman, 2020). Specifically, features like leaf area, length, perimeter, width, and colour can be employed to differentiate between plants and inform plant management strategies (Speck & Speck 2021). Despite these challenges, significant progress has been made in developing object recognition algorithms for precision agriculture, with varying degrees of accuracy achieved in different applications. The application of deep learning techniques has demonstrated considerable potential in achieving these objectives. Over the past decade, deep learning has transformed the field of image processing, achieved unprecedented success, and found numerous practical applications in precision agriculture. While large datasets are essential for training and validating deep learning algorithms, advances in computational power and data availability have made them increasingly popular. As a subset of machine learning, deep learning leverages hierarchical representations of data through sequential layers, typically employing convolutional neural networks (CNNs) to extract complex, non-linear image features. This approach has been shown to exhibit exceptional generalisation capabilities, making it well-suited for classification tasks (Saedi & Rezaei, 2024). This task begins with the input of an image, which can vary in size, and undergoes pre-processing before entering the feature extraction stage. This phase involves a series of layers that progressively extract features from the image, with the complexity of the features increasing with each additional layer. Following feature extraction, the classification process begins, employing traditional fully connected layers commonly found in neural networks. The arrangement and configuration of these layers give rise to a diverse range of networks with distinct characteristics and capabilities (Chollet, 2017).

Convolutional neural networks have been extensively explored for identification and classification tasks in agriculture. Research has demonstrated the effectiveness of these networks in various applications. For instance, Saedi and Khosravi (2020) developed an image-based CNN model to recognise six different types of on-branch fruits in orchards, achieving an impressive accuracy of 99.8%. Additionally, Khosravi, Saedi, and Rezaei (2021) developed a CNN model to classify olive fruit at different cultivars and developmental phases, attaining 91% classification. Furthermore, researchers have used deep neural networks such as Xception (Salim, Saeed, Basurra, Qasem, & Al-Hadhrami, 2023) and lightweight CNNs (Saedi, Rezaei, & Khosravi, 2024), to recognise and classify fruits with high accuracy, demonstrating the potential of these models in image classification tasks.

Deep learning algorithms have been successfully applied to weed detection and classification, demonstrating superior performance in distinguishing between crop plants and weeds (Li *et al.*, 2024). For instance, Quan *et al.* (2019) employed the Faster R-CNN model to detect corn seedlings and weeds in complex environments, while Fan, Chai, Zhou, and Sun (2023) improved this model to achieve an accuracy of over 98.43% in identifying weeds in cotton fields. Other studies have utilised deep learning-based models to identify common weeds in sugar beet cultivation (Nasiri, Omid, Taheri-Garavand, & Jafari 2022), discriminate pepper from weeds (Subeesh *et al.*, 2022), and detect weeds in sugar beet fields (Gao *et al.*, 2020). Additionally, researchers have evaluated the performance of deep learning models such as Yolov8, Yolov9, and customised Yolov9 under real-field conditions for eight crop species (GC, Zhang, Howatt, Schumacher, & Sun, 2024). Similarly, a modified Xception deep learning approach was successfully utilised to distinguish saffron from its broadleaf weeds, yielding promising results with F1 scores ranging from 91% to 96% (Makarian & Saedi, 2024). In a practical study, Rai and Sun (2024) designed a single-stage deep learning architecture that accomplishes two tasks simultaneously: detecting weed presence through bounding boxes and achieving pixel-wise instance segmentation on unmanned aerial systems (UAS) acquired remote sensing images. The model achieved the best detection and segmentation scores of 85.4% and 82.1%, respectively.

The aforementioned studies illustrate the potential of deep learning algorithms for plant identification and emphasise the necessity for further research, particularly in the area of weed-plant discrimination. In this context, this study employs advanced deep learning models with colour images to accurately distinguish winter wheat from four common weed species, providing a foundation for developing precise and automated weed management systems in winter wheat fields. To find a suitable deep learning model for our study, we considered four advanced deep neural network models-Xception, EfficientNetB0, VGG19, and InceptionResNetV2—among the state-of-the-art structures as backbone networks to develop improved models. The research findings provide the groundwork for developing mobile apps or robotic weeders that facilitate site-specific weed management, aiming to reduce herbicide use and environmental impact while enhancing wheat yield and quality.

Materials and Methods

Image Preparation

To address the requirements of the study, 542 images were collected from five classes: Winter Wheat (*Triticum aestivum* L.), Annual Bugloss (*Anchusa arvensis* L.), Bastard Cabbage (*Rapistrum rugosum* L.), Hoary Cress (*Cardaria draba* (L.) Desv.), and Flixweed (*Descurainia sophia* L.). Figure 1 illustrates a selection of these images. The photos were taken with the 48-megapixel camera of an A12 Samsung Galaxy phone (SM-A125F/DS).

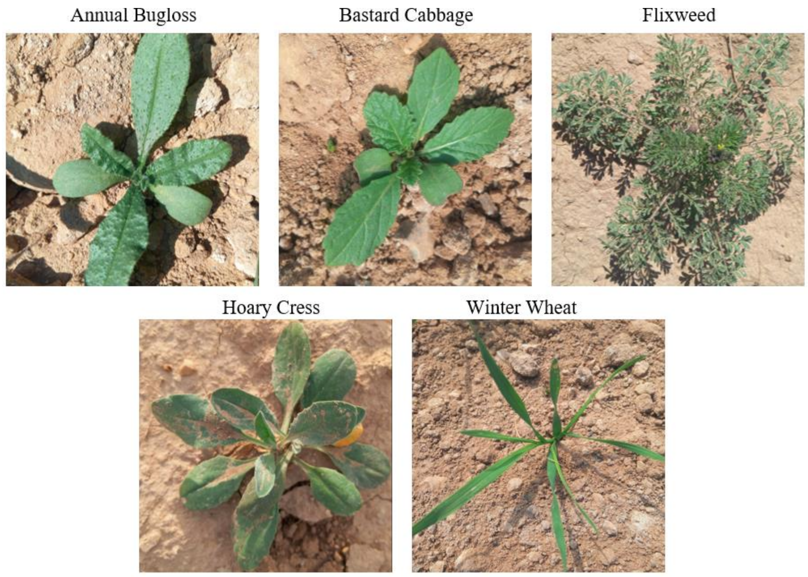

Fig. 1. Images of winter wheat and four weeds showcasing the five classes studied under natural conditions within a field

In the pie chart shown in Figure 2, the quantity and proportion of samples for each class are shown. The illustration highlights the balanced distribution of data used in this study. Having a balanced dataset is crucial to prevent bias, improve generalisation, enhance performance, promote stability, and avoid misinterpretation. This balance ensures that the model receives sufficient examples from each class, enabling effective learning and accurate predictions across all classes.

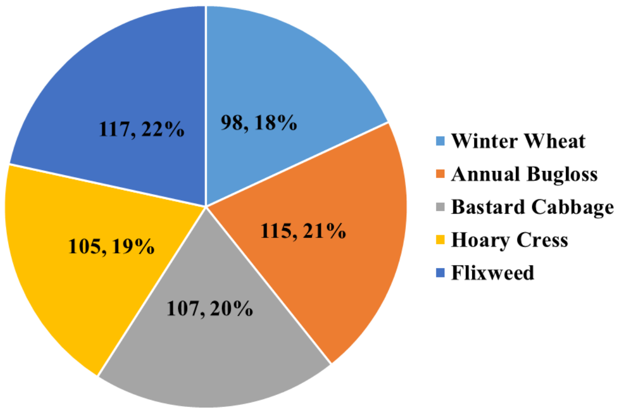

Fig. 2. The pie chart for the number and proportion of samples showcases a balanced distribution of data used in this study

The images captured underwent a review process in which inappropriate samples were excluded. An agronomist with expertise in weed and crop properties contributed to this selection process. Ultimately, 542 images were chosen to develop the model and train the network. The selected images were divided into three datasets: training, validation, and testing. Eighty percent of the data was allocated for training, while the remaining 20% was used for testing. Within the training data, 15% was set aside for validation purposes. It is worth emphasising that the test set is reserved exclusively for evaluating the final model's performance and testing its accuracy on unseen data. This separation ensures a reliable assessment of the model's generalisation capabilities.

Image Pre-processing

Pre-processing input images is essential for improving the model's accuracy, mitigating overfitting, and enhancing its generalisation ability.

Resize and Normalisation

Initially, we standardised the image sizes to 299 × 299 pixels to ensure uniform resolution across all images. Subsequently, we normalised the resolutions to fall within the range [0,1] by utilising Equation 1:

$$x_i' = \frac{x_i - x_{min}}{x_{max} - x_{min}} \qquad (1)$$

where x_i' symbolises the normalised value within the dataset, x_i represents the i^{th} value in the dataset, and x_{min} and x_{max} denote the minimum and maximum values in the dataset, respectively. This formula guarantees that after normalisation, the normalised value for the dataset's minimum value will consistently be 0, and the normalised value for the dataset's maximum value will invariably be 1.

Augmentation

Data augmentation is a widely recognised method in computer vision. It seeks to create extra training data from existing samples by applying random transformations. This is crucial when datasets are small, as limited data can lead to overfitting and poor generalisations. Augmentation addresses this scarcity by creating variations, allowing models to learn invariant features, ultimately improving performance on unseen data despite the original dataset's size limitations. This technique ensures that the generated images are realistic and that each specific image is unique (Chollet, 2017). Consequently, image augmentation can alleviate the challenges encountered by deep neural networks regarding their reliance on a substantial quantity of annotated data, leading to improved accuracy. The extensive dataset enhances the training procedure by allowing the network to acquire all essential parameters while reducing the likelihood of overfitting. In the present study, an automated data augmentation technique was utilised, incorporating random height and width shifts, random flipping, random contrast adjustments, and random rotations. Table 1 represents the specific data augmentation arguments for our task.

Table 1- Augmentation parameters and values

Image augmentation parameters	Values
Random height translation	0.1
Random width translation	0.1
Random flip	True
Random contrast	0.15
Random rotation	0.15

Candidate Models

Backbone Networks

The initial step in reaching our goal is to select a backbone network from several choices through transfer learning, which entails loading weights from the ImageNet dataset. To this end, we tested four innovative standard deep learning networks, including Xception, EfficientNetB0, VGG19, and InceptionResNetV2.

Fine-Tuning

The objective of this fine-tuning process was to customise the candidate backbone networks for the dataset and task at hand, leveraging the previously learned features while adapting to the new data. This technique prevents overfitting in pre-trained layers while facilitating the adaptation of the newly added layers to the new data. During the fine-tuning process, our goal was to selectively freeze certain layers (the earlier ones) while enabling the training of others (the later ones) when incorporating a pre-trained model into transfer learning within a deep learning framework. Initially, we disabled the trainable attribute for the first 20 layers, locking them during training to prevent their weights from being altered and preserving the valuable features they had already acquired from the original training data. Subsequently, we proceeded to fine-tune the later layers of the backbone model. We then iterated through the layers starting from the 20th position and activated the trainable attribute for each of these layers. This adjustment allows these layers to undergo training and updates throughout the training phase.

Modifying Block

To develop a robust CNN model, we added a modifying block to the last layer of the proposed backbone networks. We tested various layer configurations for the modifying block, exploring different types, placements, and parameters to find the most efficient setup. This included examining combinations of 2D Convolution, Batch Normalisation, Dropout, and Global Average Pooling layers. Parameters were selected through experimentation testing, though the specifics are not detailed here for the sake of brevity. Consequently, the optimised modifying block involved three sets of layers, including Convolution, Batch Normalisation, Max Pooling, and Dropout, followed by the Fully Connected and Global Average Pooling layers. The final layer of the candidate networks was supplemented with these additional layers to develop the proposed architectures in this study (Fig. 3).

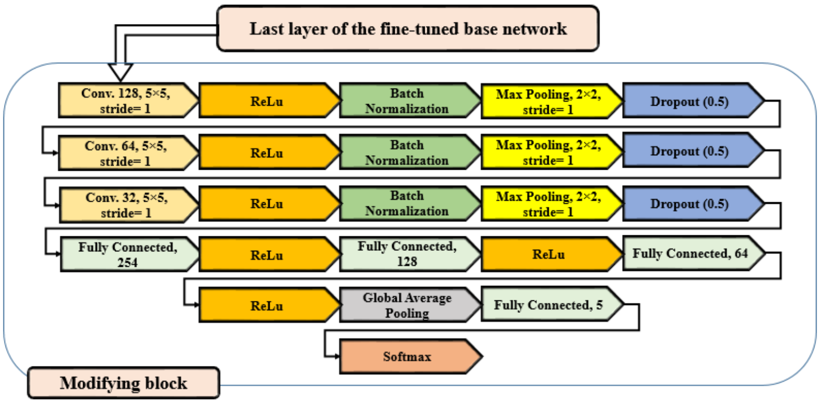

Fig. 3. Modifying block appended to the final layer of the backbone networks

By following the steps outlined earlier, we developed four distinct models–improved Xception, improved EfficientNetB0, improved VGG19, and improved InceptionResNetV2–that were labelled Model 1 through Model 4, respectively. Subsequently, we evaluated these models, using images resized to 299×299 pixels, the SGD optimiser, a batch size of 32, and 200 epochs to identify the optimal model. During this process, we employed selection criteria that included assessing the model's stability during training, as well as analysing test accuracy and test loss.

The detailed outcomes of this step, including a comparison of the models' performance, are presented in Section 3.2. Figure 4 summarises the proposed model for our study.

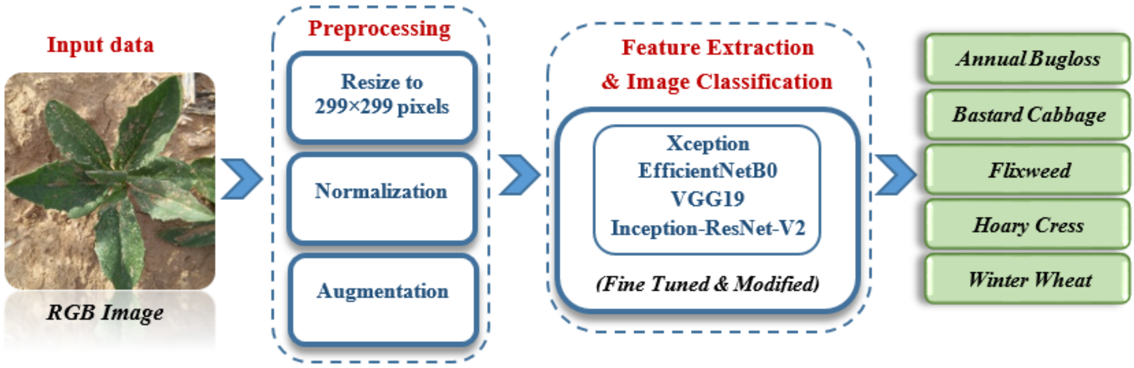

Fig. 4. Deep learning structure for the classification of five plant species under study

Following the evaluation of the candidate standard networks, the Inception-ResNetV2 stood out as the top performer based on the specified selection criteria (see Results and Discussion, Evaluation of Models section). Therefore, we focus on the detailed structure of this network.

Inception-ResNetV2, a cutting-edge deep learning architecture developed by Google, combines the Inception and ResNet modules to enhance performance in image recognition tasks. Renowned for its exceptional accuracy and efficiency in handling intricate visual data, this architecture integrates key elements, such as the Inception module (GoogLeNet) for capturing multi-scale features and the ResNet-inspired residual connections that aid gradient flow during training. Additionally, Inception-ResNetV2 introduces Inception-ResNet blocks, merging Inception and ResNet principles, to create powerful feature extraction mechanisms using convolutional layers of varying sizes and depths. By incorporating parallel paths within each module, the network explores diverse ways to represent input data, achieving a richer feature set and boosting overall recognition capabilities while maintaining efficient computation without compromising accuracy. This network consists of various types of layers, including Average Pooling, Dropout, Inception-ResNet-v2-A, Inception-ResNet-v2-B, Inception-ResNet-v2-C, Inception-ResNet-v2 Reduction-B, Reduction-A, and Softmax (Fig. 5). These layers serve different functions within the network, such as pooling operations, regularisation, image model blocks, and output functions. It has a total of 467 layers. This extensive depth in the network contributes to its ability to handle complex image classification tasks effectively.

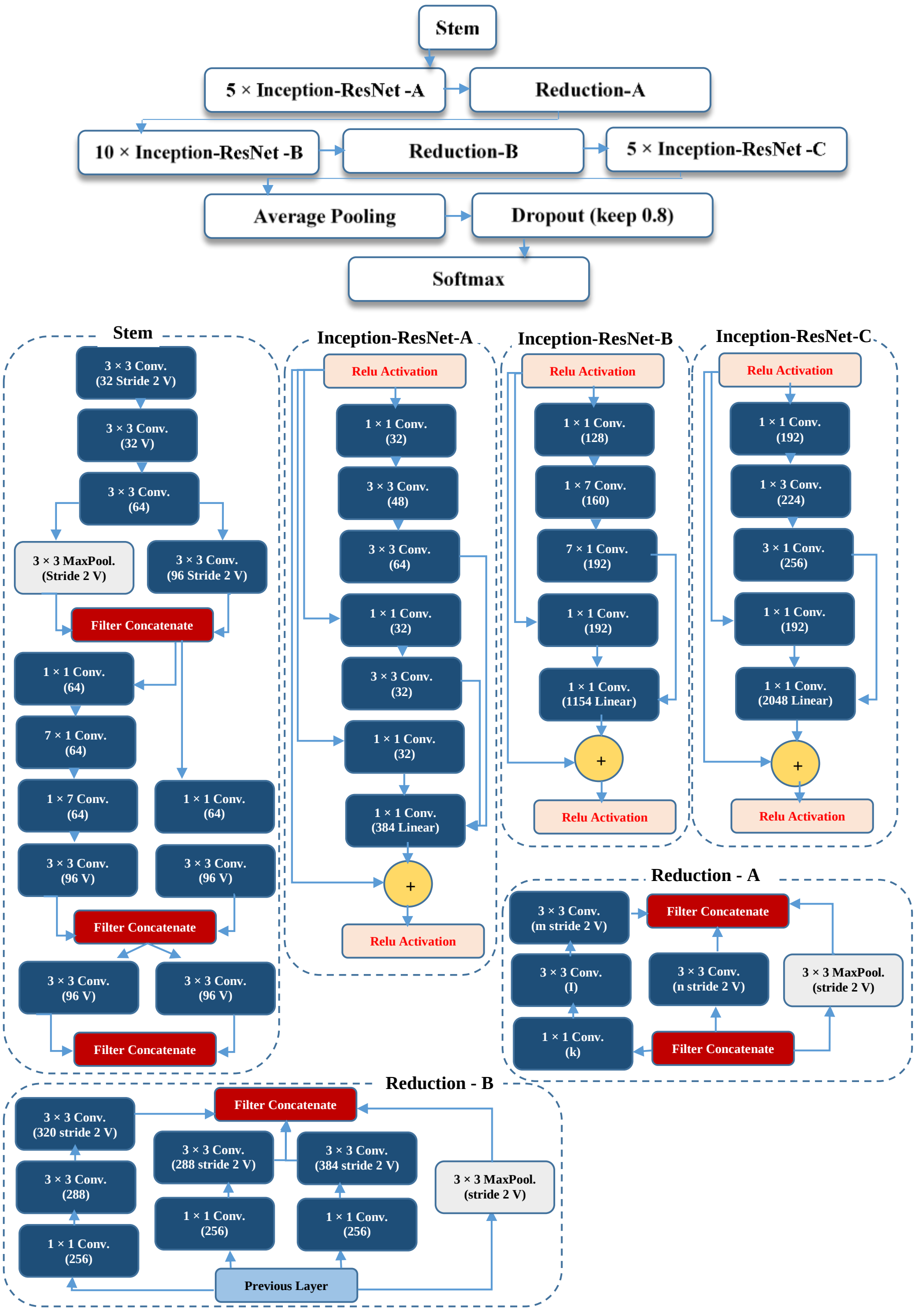

Fig. 5. The architecture of the Inception-ResNet-V2 deep learning network

Figure 6 offers a comprehensive overview of the layers comprising the best model (Inception-ResNet-V2 – based network), including the output shapes and parameter count. The model includes approximately 24,000 (0.42%) non-trainable parameters, from a total exceeding 59 million. Specific layers, such as Dropout, Max Pooling, and Global Average Pooling, do not add to the number of trainable parameters. This is because these layers do not include any trainable parameters themselves.

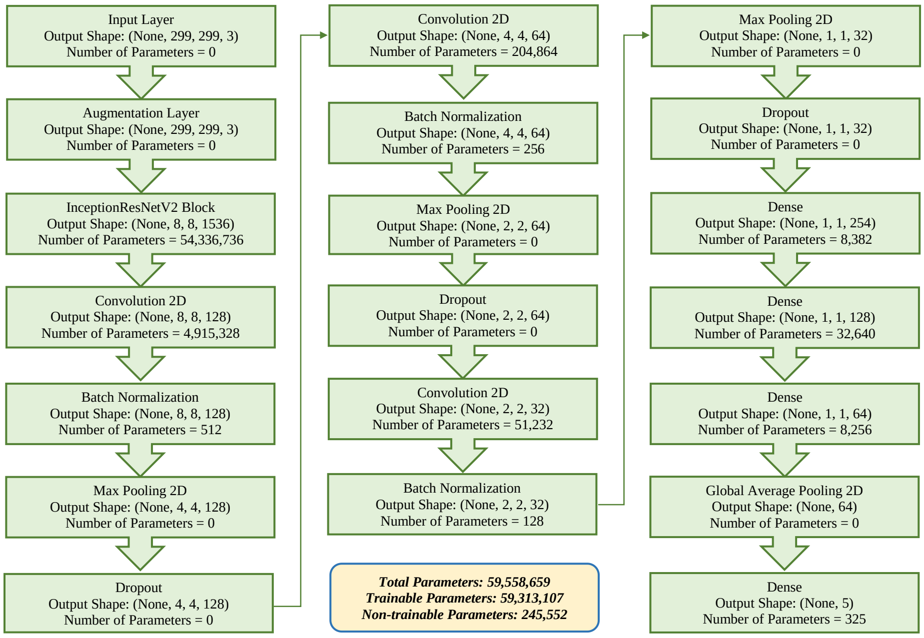

Fig. 6. Layer configuration of the improved InceptionResNetV2 deep learning model

Network Training

The training of the CNNs involves two main stages: Feed-Forward and Back Propagation. In the feed-forward phase, the network evaluates its output against the labelled output to assess errors. During backpropagation, gradients are calculated from this error, updating the weight matrices. The input is processed through layers, and the resulting output is compared to the desired output to determine and minimise errors through iterative adjustments over multiple epochs. The error calculation involves various formulas and functions, and the optimisation process consists of incremental adjustments to the weights to minimise errors. To achieve this goal, we chose the appropriate optimiser from options such as SGD, RMSprop, Nadam, and Adam. The performance of the model was evaluated using test accuracy and test loss. We additionally utilised the categorical cross-entropy loss function for the image data in this research. Table 2 represents the detailed properties of the optimisers.

Table 2- The properties of the optimisers used in this study

Optimiser	Properties
RMSprop	lr = 0.001
SGD	lr = 0.001, momentum = 0.5, nesterov = FALSE
Adam	lr = 0.001, beta_1 = 0.9, beta_2 = 0.999
Nadam	lr = 0.001, beta_1 = 0.9, beta_2 = 0.999

The training of the model entailed a systematic exploration of hyperparameters and components to determine the optimal configuration. During the training process, we carefully monitored the loss and accuracy trends for both the training and validation datasets at each epoch. This rigorous method enabled us to comprehensively evaluate the performance of the models and decide on their efficiency for our goal.

The process of selecting the best model is depicted in the results and discussion section. To evaluate the potential models, we analysed several performance metrics, including accuracy, loss, and model stability. Accuracy measures the proportion of correct predictions made by the model, while loss indicates the average error for each instance. Generally, lower loss values suggest better model performance. However, it is essential to recognise that a model exhibiting high accuracy but significant loss may be at risk of overfitting, which can adversely affect its ability to generalise to unseen test data. So, we meticulously assessed the possibility of overfitting during our comparative analysis of the four candidate models.

To guarantee the dependability and reproducibility of our findings, we conducted the training, validation, and testing phases using Python version 3.10.12 on the Google Collaboratory platform. The computational environment features an NVIDIA K80 GPU with 12 GB of memory, and we utilised Keras with TensorFlow as the backend (version 2.15.0), alongside libraries such as OpenCV, to conduct the experiments.

Results and Discussion

The results of developing deep learning models for distinguishing between winter wheat and its four prevalent weeds, namely annual bugloss, bastard cabbage, hoary cress, and flixweed, using colour images, are presented in this section. These models can be suitable for precision wheat weed management in various scenarios where any of these weeds are present.

Evaluation of Models

The first stage in developing an appropriate deep learning model entails the selection of a backbone network from a variety of standard options via transfer learning, where the initial weights are imported from the ImageNet dataset. We assessed four cutting-edge standard deep learning networks: Xception, EfficientNetB0, VGG19, and InceptionResNetV2. Following fine-tuning, these networks underwent a modification phase by incorporating three blocks of CNN layers into the ultimate layer of the fine-tuned standard candidate models to establish four candidate architectures (Model 1 to Model 4). The models were trained using images resized to 299 × 299 pixels, with the SGD optimiser, a batch size of 32, and 200 epochs to determine the optimal network. During this process, we employed selection criteria that assessed model stability during training and analysed test accuracy and test loss.

The results comparing the four candidate models based on maximum and minimum accuracy on the training, validation, and test datasets are presented in Table 3. As observed in this table, Models 1 and 4 achieved 100% accuracy on the training dataset, while Model 3 attained 100% accuracy on the validation dataset. Notably, Model 3 produced the lowest loss values among all models on the training, validation, and test datasets. However, Model 4 achieved the highest accuracy on the test dataset, followed by Models 1 and 3, respectively. Model 2 yielded the lowest test accuracy. The accuracy and loss values of Models 1 and 4 are relatively close, which could be attributed to the presence of the Inception module in both models.

Table 3- Comparison of the four deep learning models on training, validation, and test datasets

	Model 1	**Model 2**	**Model 3**	**Model 4**
Maximum accuracy on train dataset	1.0000 (epoch: 161)	0.9837 (epoch: 179)	0.9810 (epoch: 190)	1.0000 (epoch: 179)
Minimum loss on train dataset	3.1821 (epoch: 200)	3.2169 (epoch: 200)	2.9758 (epoch: 200)	3.1642 (epoch: 199)

Maximum accuracy on validation dataset	0.9846 (epoch: 187)	0.9077 (epoch: 194)	1.0000 (epoch: 161)	0.9846 (epoch: 188)
Minimum loss on validation dataset	3.2592 (epoch: 198)	3.4446 (epoch: 194)	2.9286 (epoch: 200)	3.2194 (epoch:197)
Accuracy on test dataset	0.9725	0.8532	0.9358	0.9817
Loss on test dataset	3.2550	3.4555	2.9868	3.1933

To gain deeper insights into the training process of the four candidate models, we analysed the trends of accuracy and loss concerning the number of epochs during the training phase for both the training and validation datasets. The graphical representation of these trends for all models is depicted in Figure 7. The learning curves indicate consistent convergence behaviour and comparable training–validation trends under the reported experimental setup. Model 2 exhibits slightly more pronounced fluctuations compared to the other three models, indicating a less stable training pattern. In contrast, Models 1, 3, and 4 display a consistent downward trend in losses and a steady increase in accuracy, with only minor variations. This behaviour indicates that Models 1, 3, and 4 exhibit greater resistance to instability and are likely to generalise more effectively to new, unseen data, rendering them more dependable options.

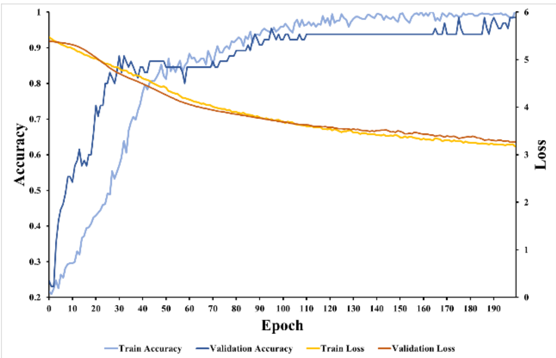

Model 1

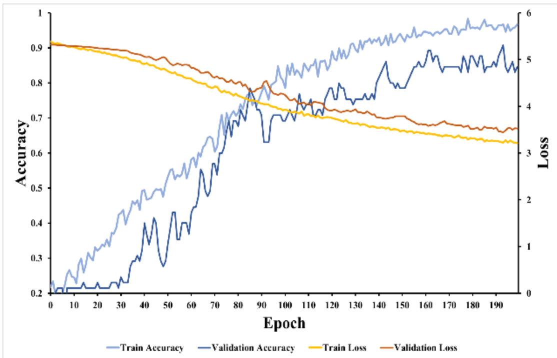

Model 2

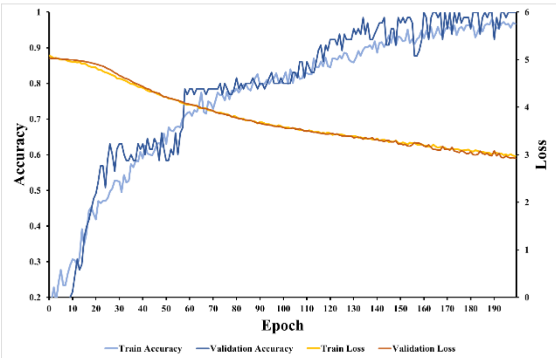

Model 3

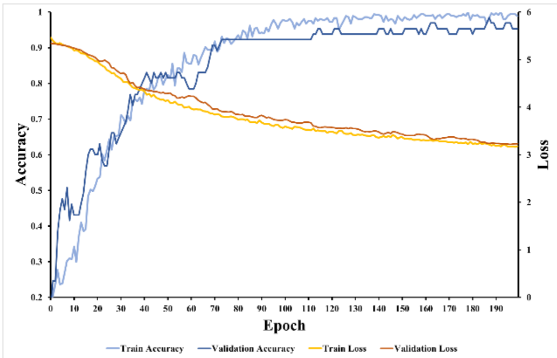

Model 4

Fig. 7. Accuracy and loss trends on train and validation datasets for the four-candidate model during training

Figure 8 compares the total parameters, trainable parameters, and non-trainable parameters for the four candidate models. This comparison provides valuable insights into the response time of the models. According to this figure, Model 1 and Model 4 exhibit comparable values for these parameters, which can be attributed to their Inception-based architectures. Model 2 offers the minimum number of trainable parameters, making it advantageous in terms of response time for real-time applications. However, it achieves the lowest accuracy and the highest loss on test datasets among all four models. Model 3, on the other hand, provides promising results in terms of accuracy and loss while maintaining a reasonable number of trainable parameters (Figure 8), making it a compelling choice for our purposes.

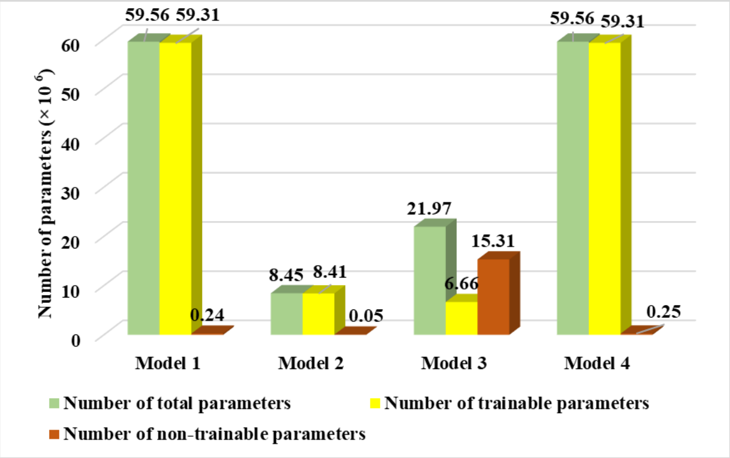

Fig. 8. Evaluation of the number of parameters (total, trainable, and non-trainable) for the four candidate models

After carefully considering the evaluation criteria, we proposed Model 4 as the optimal choice for our specific purpose. This model utilises a modified and fine-tuned InceptionResNetV2 architecture with the SGD optimiser. Model 4 exhibited minimal fluctuations during the training process, indicating a high level of stability. Moreover, it achieved impressive accuracy and loss values on the test dataset (98.17% accuracy and a loss of 3.19, respectively), along with a reasonably fast response time. These factors suggest that Model 4 would perform exceptionally well in real-world scenarios, making it our preferred selection.

Classification Performance

To evaluate the efficacy of the models in distinguishing the five classes, various parameters were considered. These parameters include True Positive (TP), representing the count of instances correctly identified as positive; True Negative (TN), denoting instances correctly identified as negative; False Positive (FP), indicating instances incorrectly identified as positive; and False Negative (FN), signifying instances incorrectly identified as negative. These parameters are utilised in the development of two classification metrics: the classification report and the confusion matrix. The classification report provides insights into the model's performance based on precision, recall, and F1-score, as outlined in Equations 2-4. Precision quantifies the model's accuracy in predicting positive cases. A high precision value suggests a lower ratio of incorrect to correct predictions, and conversely. Recall quantifies the ratio of accurately predicted positive instances to the total number of actual positive instances, highlighting the model's capability to correctly identify all positive instances. Furthermore, recall provides information on the model's capacity to minimise false negatives. The F1-score, calculated as the geometric mean of precision and recall, serves as a metric that balances these two parameters to achieve an optimal trade-off between precision and recall.

$$Precision = \left(\frac{TP}{TP + FP}\right) \tag{2}$$

$$Recall = \left(\frac{TP}{TP + FN}\right) \tag{3}$$

$$f1 - score = \left(2 \times \frac{Precision \times Recall}{Precision + Recall}\right) \tag{4}$$

The classification report describing the categorisation of winter wheat, annual bugloss, bastard cabbage, hoary cress, and flixweed classes by colour images through the four models is outlined in Table 4.

Table 4- The classification report detailing the recognition performance of the five classes by the four candidate models

		Annual Bugloss	Bastard Cabbage	Flixweed	Hoary Cress	Winter Wheat	Micro Avg.	Macro Avg.	Weighted Avg.	Samples Avg.
Precision	Model 1	0.95	0.95	1.00	0.95	1.00	0.97	0.97	0.97	0.96
	Model 2	0.74	1.00	1.00	1.00	0.83	0.88	0.92	0.91	0.84
	Model 3	1.00	0.80	1.00	1.00	1.00	0.95	0.96	0.96	0.93
	Model 4	0.95	0.95	1.00	1.00	1.00	0.98	0.98	0.98	0.97
Recall	Model 1	0.91	0.95	1.00	1.00	0.95	0.96	0.96	0.96	0.96
	Model 2	1.00	0.52	0.96	0.71	1.00	0.84	0.84	0.84	0.84
	Model 3	0.70	0.95	1.00	1.00	1.00	0.93	0.93	0.93	0.93
	Model 4	0.91	1.00	1.00	1.00	0.95	0.97	0.97	0.97	0.97
F1-score	Model 1	0.93	0.95	1.00	0.98	0.97	0.97	0.97	0.97	0.96
	Model 2	0.85	0.69	0.98	0.83	0.91	0.86	0.85	0.86	0.84
	Model 3	0.82	0.87	1.00	1.00	1.00	0.94	0.94	0.94	0.93
	Model 4	0.93	0.98	1.00	1.00	0.97	0.98	0.98	0.98	0.97
Supports		23	21	24	21	20	109	109	109	109

Based on Table 4, the precision parameter analysis reveals that Model 1 was able to identify the flixweed and winter wheat classes with 100% accuracy. Using Model 2, three classes namely bastard cabbage, flixweed, and hoary cress, were identified with 100% accuracy. Moreover, Model 3 successfully identified four classes including annual bugloss, flixweed, hoary cress, and winter wheat, with 100% accuracy, while Model 4 detected three classes i.e. flixweed, hoary cress, and winter wheat, with 100% precision. On the other hand, if the objective is to identify a specific class (e.g. for selective treatment), it is observed that annual bugloss can be accurately identified using Model 3 and bastard cabbage using Model 2, both with 100% accuracy. Furthermore, Models 2, 3, and 4 can be utilised to identify hoary cress with 100% accuracy. It is worth noting that flixweed can be identified accurately with 100% precision by all four models. Conversely, if the goal is to differentiate weed species from winter wheat for herbicidal purposes, Models 1, 3, and 4 can be employed to identify winter wheat with 100% precision. Lastly, based on the aforementioned table, the lowest precision value was related to identifying annual bugloss with Model 2 (0.74). To evaluate the models' capacity to minimise false negatives, we can compare their recall values. The recall values in the table indicate that this parameter achieved 100% for the annual bugloss class using Model 2; for the bastard cabbage class using Model 4; for the flixweed and hoary cress classes using Models 1, 3, and 4; and for the winter wheat class using Models 2 and 3. Conversely, the lowest recall value was observed for Model 2 in relation to the bastard cabbage class (0.52). Furthermore, the F1-score parameter reached 100% for the flixweed class using Models 1, 3, and 4; for the hoary cress class using Models 3 and 4; and for the winter wheat class using Model 3. The lowest F1-score value was observed for the bastard cabbage class using Model 2 (0.69). Consequently, Model 4 demonstrated the best performance with the highest average precision, recall, and F1-score values.

Figure 9 presents the confusion matrices for classifying five categories with four candidate models. The rows represent the true classes, while the columns show the predicted classes. Through these matrices, we can see that there were only two annual bugloss instances mistakenly classified as bastard cabbage or hoary cress using Model 1. Additionally, Models 3 and 4 misclassified seven and one annual bugloss instances as bastard cabbage, respectively, whereas Model 2 accurately identified this class with no errors. For the bastard cabbage class, one instance was misclassified as annual bugloss using Model 1; eight instances were misclassified as annual bugloss using Model 2; and one instance was misclassified as winter wheat, also using Model 2. In contrast, Models 3 and 4 accurately classified this class with 100% precision. The flixweed class was accurately classified without error using Models 1, 3, and 4; however, Model 2 misclassified one instance as winter wheat. For the hoary cress class, Models 1, 3, and 4 accurately classified it without error; whereas Model 2 misclassified two instances as annual bugloss and four instances as winter wheat. Finally, for the winter wheat class, Models 1, 2, and 3 accurately classified it without error; whereas Model 4 misclassified only one instance as annual bugloss.

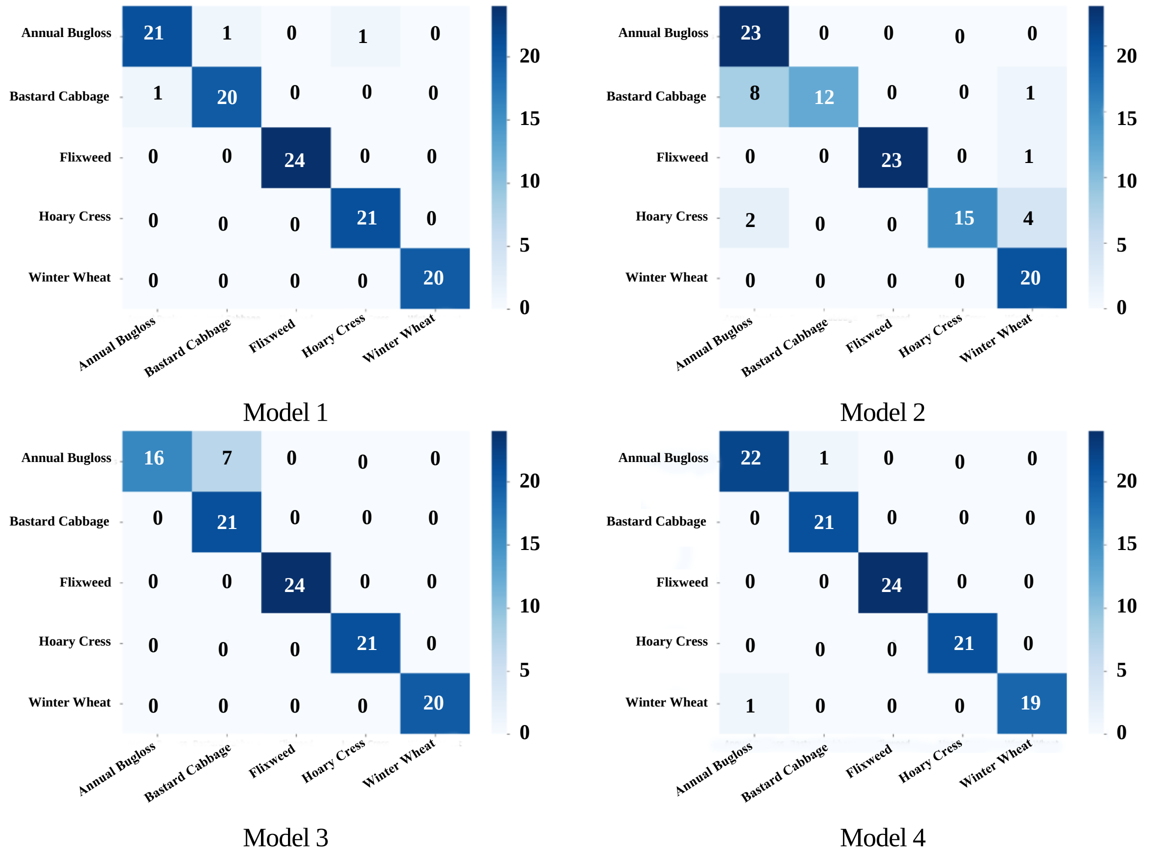

Fig. 9. Confusion matrices illustrating the classification performance of the five classes using the four developed models

Winter Wheat Weed Management Scenarios

It is essential to emphasise that the findings of this study can be effectively generalised to encompass various scenarios in winter wheat fields with respect to weed appearance. Given that four distinct weed species have been investigated, we can conclude that the proposed model(s) can be utilised as a tool for efficient weed management in 15 different weed appearance scenarios that may arise in winter wheat fields. These scenarios are detailed in Table 5, which accounts for one to four weeds that can coexist alongside winter wheat. Notably, scenario 15 represents the general condition that we have studied in this investigation.

Table 5- Fifteen scenarios for different weed appearances in winter wheat fields

Scenario	Weed(s) alongside winter wheat	No. of classes
Scenario 1	Flixweed	2
Scenario 2	Hoary Cress	2
Scenario 3	Annual Bugloss	2
Scenario 4	Bastard Cabbage	2
Scenario 5	Flixweed + Hoary Cress	3
Scenario 6	Annual Bugloss + Flixweed	3
Scenario 7	Bastard Cabbage + Flixweed	3
Scenario 8	Annual Bugloss + Hoary Cress	3
Scenario 9	Bastard Cabbage + Hoary Cress	3
Scenario 10	Annual Bugloss + Bastard Cabbage	3
Scenario 11	Annual Bugloss + Flixweed + Hoary Cress	4
Scenario 12	Bastard Cabbage + Flixweed + Hoary Cress	4
Scenario 13	Annual Bugloss + Bastard Cabbage + Flixweed	4
Scenario 14	Annual Bugloss + Bastard Cabbage + Hoary Cress	4
Scenario 15	Annual Bugloss + Bastard Cabbage + Flixweed + Hoary Cress	5

For this analysis, we used confusion matrices (Figure 9), and for each scenario, we extracted a separate subset that must include winter wheat for each model. This analysis will involve creating 60 subsets of the confusion matrices (15 subsets for each model). The results of this analysis are presented in Table 7 and Figure 10. Accordingly, it was concluded that Models 1, 3, and 4 are usable with 100% accuracy for scenarios 1, 2, 4, 5, 7, 9, and 12. Scenario 3 can be treated with 100% accuracy using Models 1, 2, and 3. Additionally, for scenario 6, Models 1 and 3 are suggested with 100% accuracy. For scenario 8, Model 3 will perform best with 100% accuracy. For scenario 11, Model 3 showed the best performance (100%). For scenarios 10, 13, and 14, while 100% accuracy was not achieved, Models 1 and 4 provided the highest accuracy of around 97% for scenario 10. The same two models can be used for scenario 13, with an accuracy of about 98%. Model 4 can be employed for scenario 14 with an accuracy of 98%. If we were to choose a comprehensive model for various scenarios, we would consider the average accuracy across different models and scenarios. Accordingly, based on Table 6, Model 4 has the highest average accuracy (98.92%) and the lowest standard deviation (0.0110), making it the most suitable model. Although Model 3 is noteworthy for achieving 100% accuracy in 11 different scenarios. It is important to reiterate that scenario 15 is the initial and overall scenario considered in this research, based on which the deep learning models have been designed.

Table 6- Average and standard deviation of accuracies for the four models in all scenarios

	Model 1	Model 2	Model 3	Model 4
Average accuracy in all scenarios	0.9890	0.9191	0.9776	0.9892
STD of accuracy in all scenarios	0.0161	0.0504	0.0380	0.0110

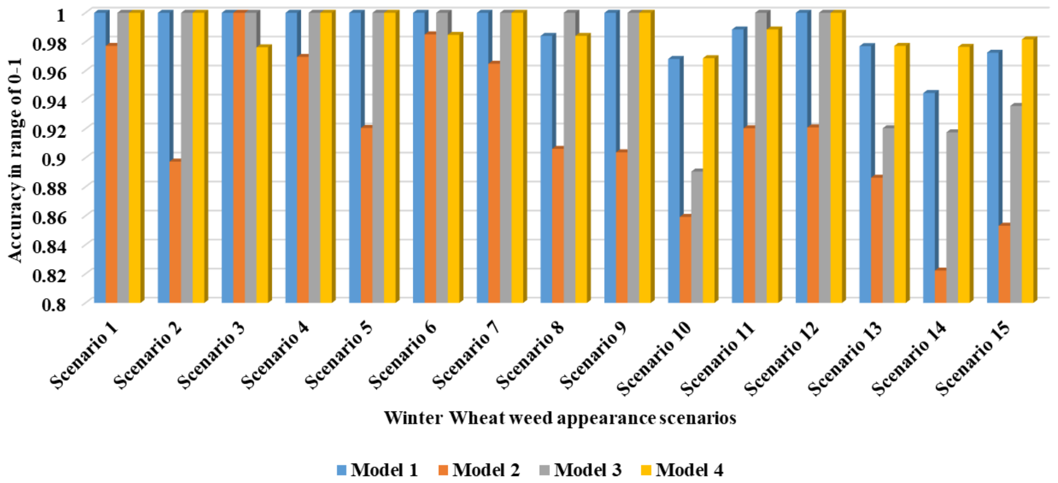

Fig. 10. The accuracy of the four model candidates in different winter wheat weed appearance scenarios.

The present study demonstrated the effectiveness of deep learning models in distinguishing winter wheat from four prevalent weed species: annual bugloss, bastard cabbage, hoary cress, and flixweed, using RGB colour images. Among the four candidate architectures developed through transfer learning and fine-tuning, the modified InceptionResNetV2 (Model 4) achieved the best overall performance, with a test accuracy of 98.17%, minimal loss, and stable training behaviour. Importantly, the evaluation of the models across 15 different weed appearance scenarios further emphasised the robustness of Model 4, which exhibited the highest mean accuracy (98.92%) and the lowest standard deviation (0.0110). These findings suggest that this model is particularly well-suited for precision weed management in winter wheat fields under diverse and dynamic conditions. Our approach aligns with established practices for small-dataset plant classification, where transfer learning from ImageNet-pretrained models combined with augmentation effectively mitigates overfitting (Batchuluun, Nam, & Park, 2022; Sultan, Chowdhury, Jahan, & Dunren, 2025; Richter & Kim, 2025).

Furthermore, our results are consistent with and extend previous work in the field. Shao *et al.* (2023) applied a lightweight YOLOv5s-based framework for weed recognition in paddy fields and reported robust but lower accuracy under natural conditions compared with our findings. Similarly, GC *et al.* (2024) tested five deep learning frameworks to classify 14 weed and crop species in greenhouse environments, but their reported performance was relatively limited due to high inter-class similarity. Makarian and Saedi (2024) achieved near-perfect accuracy for weed discrimination under natural conditions; however, their model was constrained by a small number of classes, limiting generalisability. In contrast, our study addressed a greater number of weed species and multiple coexistence scenarios, thereby providing a more comprehensive framework for real-world applications. The scenario-based analysis is of particular importance. By evaluating model performance across 15 distinct weed–crop combinations, we demonstrated that deep learning models can be adapted for various field conditions, including cases with one to four competing weed species. This scenario-driven approach strengthens the practical applicability of the models, as farmers and agronomists are often faced with heterogeneous weed infestations. Notably, while Model 3 achieved 100% accuracy in 11 scenarios, Model 4 combined superior stability, high average accuracy, and low variance, making it the most reliable model overall.

From a broader perspective, these results confirm that deep learning methods can effectively support precision agriculture by enabling selective and automated weed management. Nevertheless, several challenges remain, including the need for larger and more diverse datasets, validation under varying geographical and environmental conditions, and computational efficiency for deployment on edge devices. Recent studies have highlighted the potential of multimodal imaging (e.g. RGB combined with depth or hyperspectral data) to further improve weed–crop discrimination accuracy (Li *et al.*, 2024; Xu, Zhao, Wang, & Zhang 2021). Incorporating such modalities, as well as model compression techniques for real-time applications, could be valuable directions for future research. In recent studies, multi-modal imaging approaches, combining RGB and depth information, have been proposed to improve weed detection in wheat fields under natural conditions. For instance, depth images were recoded into three-channel PHA images to enable CNN-based feature extraction, and multi-scale object detection with feature- and decision-level fusion was applied. Such methods achieved a mean average precision (mAP) of 36.1% for grass weeds, 42.9% for broadleaf weeds, and an overall detection accuracy (IoG) of 89.3% ($\alpha = 0.4$ for RGB and $\beta = 0.3$ for depth) (Xu *et al.*, 2021). While these results demonstrate the potential of multi-modal information for addressing limitations of single-modality data, several challenges remain regarding data acquisition complexity, cost, and practical applicability in real field scenarios.

In contrast, the present study demonstrates that high-performance weed detection can be achieved using only RGB images, without the need for additional depth sensors. By leveraging a modified InceptionResNetV2 architecture and carefully fine-tuned CNN layers, our proposed Model 4 achieved a test accuracy of 98.17% and demonstrated stable training behaviour with minimal fluctuations. Moreover, our approach considered four dominant weed species including annual bugloss, bastard cabbage, hoary cress, and flixweed, and evaluated performance across 15 realistic weed-crop coexistence scenarios, reflecting the diverse conditions commonly observed in wheat fields. This scenario-based evaluation highlights the generalisability and robustness of our model, which can reliably detect multiple weed species under varying field conditions. Another advantage of our study is precision at the species level. While multi-modal approaches in previous studies focused primarily on broad categories such as grass versus broadleaf weeds, our model achieved 97–100% precision and recall for individual weed species. This capability enables selective and targeted weed management, a critical requirement for precision agriculture. In addition, the streamlined use of RGB images alone reduces data acquisition costs and simplifies deployment in real-world applications, making our method more practical and scalable compared to multi-modal systems. A limitation of this study was that each model was trained once under a fixed random seed due to computational constraints. Future work should assess variance across multiple independent runs or cross-validation folds to further quantify robustness. Although the dataset size (N=542) is moderate for deep learning applications, careful validation on unseen data, detailed class-wise evaluation, and regularisation techniques were employed to mitigate overfitting. Nevertheless, additional validation through k-fold cross-validation and expansion of real-world annotated samples would further strengthen statistical robustness and generalisability.

Conclusion

In this study, four advanced deep neural network models were developed to differentiate winter wheat from four common weeds. Using colour images for training and testing, all models accurately identified the five plant species, with InceptionResNetV2 achieving the highest accuracy. Fifteen scenarios of weed presence in wheat fields were also evaluated to determine optimal weed management strategies. The models performed reliably across all scenarios, enabling targeted control of weeds without affecting wheat. The research findings provide the groundwork for developing mobile apps or robotic weeders that facilitate site-specific weed management, aiming to reduce herbicide use and environmental impact while enhancing wheat yield and quality. This approach provides a foundation for precision weed management and automated weed removal solutions.

Acknowledgements

The authors would like to acknowledge the financial support of Shahrood University of Technology for this research under project No: RP_S_219444.

Author Contributions

Seyed Iman Saedi: Software, Modelling, Methodology, Evaluation, Writing

Hassan Makarian: Conceptualisation, Data preparation; Validation; Writing

References

1. Batchuluun, G., Nam, S. H., & Park, K. R. (2022). Deep learning-based plant-image classification using a small training dataset. *Mathematics, 10*, 3091. https://doi.org/10.3390/math10173091
2. Chollet, F. (2017). *Deep learning with Python* (1st ed.). Manning Publications Co.
3. Fan, X., Chai, X., Zhou, J., & Sun, T. (2023). Deep learning-based weed detection and target spraying robot system at seedling stage of cotton field. *Computers and Electronics in Agriculture*, *214*, 108317. https://doi.org/10.1016/j.compag.2023.108317
4. Food and Agriculture Organization of the United Nations. (2021*). World food and agriculture statistical pocketbook 2021*. FAO. https://www.fao.org/documents/card/en/c/cb4592en
5. Gao, J., French, A. P., Pound, M. P., He, Y., Pridmore, T. P., & Pieters, J. G. (2020). Deep convolutional neural networks for image-based Convolvulus sepium detection in sugar beet fields. *Plant Methods*, *16*, 29. https://doi.org/10.1186/s13007-020-00570-z
6. GC, S., Zhang, Y., Howatt, K., Schumacher, L. G., & Sun, X. (2024). Multi-species weed and crop classification: Comparison using five different deep learning network architectures. *Journal of the ASABE*, *67*(2), 275-287. https://doi.org/10.13031/ja.15590
7. Gyawali, A., Bhandari, R., Budhathoki, P., & Bhattarai, S. (2022). A review on effect of weeds in wheat (*Triticum aestivum* L.) and their management practices. *Food and Agriculture Extension Review*, *34*(2), 34-40. https://doi.org/10.26480/faer.02.2022.34.40
8. Juwono, F. H., Wong, W. K., Verma, S., Shekhawat, N., Lease, B. A., & Apriono, C. (2023). Machine learning for weed–plant discrimination in agriculture 5.0: An in-depth review. *Artificial Intelligence in Agriculture, 10*, 13-25. https://doi.org/10.1016/j.aiia.2023.09.002
9. Khosravi, H., Saedi, S. I., & Rezaei, M. (2021). Real-time recognition of on-branch olive ripening stages by a deep convolutional neural network. *Scientia Horticulturae*, *287*, 110252. https://doi.org/10.1016/j.scienta.2021.110252
10. Langridge, P., Alaux, M., Almeida, N., Ammar, K., Baum, M., Bekkaoui, F., Bentley, A., Beres, B., Berger, B., Braun, H.-J., Brown-Guedira, G., Burt, C., Caccamo, M., Cattivelli, L., Charmet, G., Civáň, P., Cloutier, S., Cohan, J.-P., Devaux, P., …, & Zhang, X. (2022). Meeting the challenges facing wheat production: The strategic research agenda of the Global Wheat Initiative. *Agronomy*, *12*, 2767. https://doi.org/10.3390/agronomy12112767
11. Li, Z., Wang, D., Yan, Q., Zhao, M., Wu, X., & Liu, X. (2024). Winter wheat weed detection based on deep learning models. *Computers and Electronics in Agriculture*, *227*, 109448. https://doi.org/10.1016/j.compag.2024.109448
12. Makarian, H., & Saedi, S. I. (2024). Automated classification of saffron and broadleaf weeds of flixweed and hoary cress using deep learning and color images. *Crop Protection*, 106750.

https://doi.org/10.1016/j.cropro.2024.106750
13. Montazeri, M., Zand, E., & Baghestani, M. A. (2005). *Weeds and their control in wheat fields of Iran* (1st ed.). Agricultural Research and Education Organization Press.
14. Nasiri, A., Omid, M., Taheri-Garavand, A., & Jafari, A. (2022). Deep learning-based precision agriculture through weed recognition in sugar beet fields. *Sustainable Computing: Informatics and Systems*, *35*, 100759. https://doi.org/10.1016/j.suscom.2022.100759
15. Quan, L., Feng, H., Lv, Y., Wang, Q., Zhang, C., Liu, J., & Yuan, Z. (2019). Maize seedling detection under different growth stages and complex field environments based on an improved Faster R–CNN. *Biosystems Engineering*, *184*, 1-23. https://doi.org/10.1016/j.biosystemseng.2019.05.002
16. Rai, N., & Sun, X. (2024). WeedVision: A single-stage deep learning architecture to perform weed detection and segmentation using drone-acquired images. *Computers and Electronics in Agriculture*, *219*, 108792. https://doi.org/10.1016/j.compag.2024.108792
17. Richter, D. J., & Kim, K. (2025). Assessing the performance of domain-specific models for plant leaf disease classification: A comprehensive benchmark of transfer-learning on open datasets. *Scientific Reports*, *15*, 18973. https://doi.org/10.21203/rs.3.rs-5668089/v1
18. Sadeghi, S. H., Saedi, S. I., Peters, R. T., & Stöckle, C. (2022). Towards improving the global water application uniformity of centre pivots through lateral speed adjustment. *Biosystems Engineering*, *215*, 215-227. https://doi.org/10.1016/j.biosystemseng.2022.01.012
19. Saedi, S. I., Alimardani, R., Mousazadeh, H., & Salehi, R. (2019). Development and evaluation of an energy and water efficient intensive cropping system. *INMATEH – Agricultural Engineering*, *58*, 93-104. https://doi.org/10.35633/inmateh-58-10
20. Saedi, S. I., & Khosravi, H. (2020). A deep neural network approach towards real-time on-branch fruit recognition for precision horticulture. *Expert Systems with Applications, 159*, 113594. https://doi.org/10.1016/j.eswa.2020.113594
21. Saedi, S. I., & Rezaei, M. (2024). A modified Xception deep learning model for automatic sorting of olives based on ripening stages. *Inventions*. https://doi.org/10.3390/inventions9010006
22. Saedi, S. I., Rezaei, M., & Khosravi, H. (2024). Dual-path lightweight convolutional neural network for automatic sorting of olive fruit based on cultivar and maturity. *Postharvest Biology and Technology*, *216*, 113054. https://doi.org/10.1016/j.postharvbio.2024.113054
23. Salim, F., Saeed, F., Basurra, S., Qasem, S. N., & Al-Hadhrami, T. (2023). DenseNet-201 and Xception pre-trained deep learning models for fruit recognition. *Electronics*. https://doi.org/10.3390/electronics12143132
24. Shao, Y., Guan, X., Xuan, G., Gao, F., Feng, W., Gao, G., Wang, Q., Huang, X., & Li, J. (2023). GTCBS-YOLOv5s: A lightweight model for weed species identification in paddy fields. *Computers and Electronics in Agriculture*, *215*, 108461. https://doi.org/10.1016/j.compag.2023.108461
25. Shewry, P. R., & Hey, S. J. (2015). The contribution of wheat to human diet and health. *Food and Energy Security*, *4*(3), 178-202. https://doi.org/10.1002/fes3.64
26. Singh, M., Kukal, M. S., Irmak, S., & Jhala, A. J. (2021). Water use characteristics of weeds: A global review, best practices, and future directions. *Frontiers in Plant Science*. https://doi.org/10.3389/fpls.2021.794090
27. Speck, O., & Speck, T. (2021). Functional morphology of plants – a key to biomimetic applications. *New Phytologist*, *231*(3), 950-956. https://doi.org/10.1111/nph.17396
28. Subeesh, A., Bhole, S., Singh, K., Chandel, N. S., Rajwade, Y. A., Rao, K. V. R., Kumar, S. P., & Jat, D. (2022). Deep convolutional neural network models for weed detection in polyhouse grown bell peppers. *Artificial Intelligence in Agriculture*, *6*, 47-54. https://doi.org/10.1016/j.aiia.2022.01.002

29. Sultan, T., Chowdhury, M. S., Jahan, N., & Dunren, C. (2025). LeafDNet: Transforming leaf disease diagnosis through deep transfer learning. *Plant Direct*, *9*, e70047. https://doi.org/10.1002/pld3.70047
30. Susetyarini, E., Wahyono, P., Latifa, R., & Nurrohman, E. (2020). The identification of morphological and anatomical structures of Pluchea indica. *Journal of Physics: Conference Series*, *1539*, 012001. https://doi.org/10.1088/1742-6596/1539/1/012001
31. Xu, K., Zhao, Y., Wang, L., & Zhang, X. (2021). Multi-modal deep learning for weeds detection in wheat fields. *Frontiers in Plant Science*, *12*, 732968. https://doi.org/10.3389/fpls.2021.732968

طبقه‌بندی هوشمند علف هرز-محصول در مزارع گندم زمستانه: با رویکرد یادگیری عمیق برای کشاورزی پایدار

سید ایمان ساعدی[۱*]، حسن مکاریان[۲]

تاریخ دریافت: ۱۴۰۴/۱۱/۰۵
تاریخ پذیرش: ۱۴۰۴/۱۲/۲۴

چکیده

افزایش بهره‌وری گندم برای حفظ امنیت غذایی در سال‌های آتی یک ضرورت است. یکی از چالش‌های اصلی تولید گندم، وجود علف‌های هرز است که می‌تواند عملکرد آن را تا حد زیادی کاهش دهد. یک عامل کلیدی در تولید پایدار گندم مدیریت دقیق علف‌های هرز بر اساس طبقه‌بندی علف هرز-محصول است. برای این منظور، در مطالعه حاضر، از تصاویر رنگی و راهبردهای یادگیری عمیق برای تشخیص و تمایز گندم زمستانه از چهار علف هرز رایج آن استفاده شد که منجر به ایجاد پنج کلاس مجزا گردید. چهار شبکه یادگیری عمیق شامل Xception، EfficientNetB0، VGG19 و InceptionResNetV2 به‌عنوان شبکه‌های ستون فقرات برای برآورده کردن الزامات طبقه‌بندی تصاویر لحاظ شدند. این شبکه‌ها با استفاده از یادگیری انتقالی در ImageNet از قبل آموزش داده شدند، سپس با لایه‌های اضافی برای بهبود عملکرد در مجموعه داده‌های ما تقویت شدند. با توجه به نتایج به‌دست‌آمده، مدل بهبودیافته InceptionResNetV2 بهترین عملکرد را در بین چهار مدل نشان داد و به دقت ۹۸/۱۷٪ و خطای ۳/۱۹٪ در داده‌های آزمون دست یافت. همه مدل‌ها عملکرد بسیار خوبی در شناسایی تصاویر کلاس‌های مختلف نشان دادند، به‌طوری‌که میانگین وزنی امتیاز F1 برای مدل‌های مبتنی بر Xception، EfficientNetB0، VGG19و InceptionResNetV2 به‌ترتیب برابر با ۹۷٪، ۸۶٪، ۹۴٪ و ۹۸٪ به‌دست آمد. علاوه‌بر این، پانزده حالت متفاوت از حضور علف‌های هرز در مزارع گندم زمستانه را با تمرکز بر انواع مختلف علف‌های هرز مورد مطالعه، تجزیه و تحلیل شد تا راهبردهای موثر مدیریت علف‌های هرز با استفاده از هر یک از چهار مدل پیشنهاد داده شود. یافته‌های این تحقیق، پایه و اساسی برای توسعه برنامه‌های تلفن همراه یا وجین‌کن‌های رباتیک به‌منظور مدیریت خاص مکانی علف‌های هرز فراهم می‌آورد. این رویکرد می‌تواند در کاهش استفاده از علف‌کش‌ها و کاهش اثرات زیست‌محیطی آن و در عین حال بهبود عملکرد و کیفیت گندم نقش مهمی ایفا نماید.

واژه‌های کلیدی: تصاویر RGB، شناسایی علف‌های هرز، گندم زمستانه، یادگیری عمیق

۱- گروه آب و خاک، دانشکده کشاورزی، دانشگاه صنعتی شاهرود، شاهرود، ایران
۲- گروه زراعت و اصلاح نباتات، دانشکده کشاورزی، دانشگاه صنعتی شاهرود، شاهرود، ایران
(*- نویسنده مسئول: Email: isaedi@shahroodut.ac.ir)

https://doi.org/10.22067/jam.2026.97533.1467